A MANOVA-BASED AND OBJECT-ORIENTED STATISTICAL METHOD FOR EXTRACTION OF IMPERVIOUS SURFACE AREA

Yuyu Zhou and **Y.Q. Wang**
Department of Natural Resources Science
University of Rhode Island
Kingston, RI 02881
ilikespoon@mail.uri.edu, yqwang@uri.edu

ABSTRACT

Impervious surface area (ISA), one of the consequences of suburban sprawl, has emerged as a key indicator to explain and predict ecosystem health in relationship to watershed management. Quantifying precisely the spatial locations and distributions of ISA is essential for environmental monitoring and management. Classification of high spatial resolution remote sensing data is an important step towards obtaining ISA information. In this study, we developed a Multivariate Analysis of Variance (MANOVA)-based classification algorithm for the purpose of extracting ISA information from high spatial resolution remote sensing data. This classification algorithm took account the variability in both the training objects and the objects to be classified, as well as the correlations among different spectral bands in high spatial resolution remote sensing data. We tested the algorithm using three types of high spatial resolution imageries including true color Orthophoto, QuickBird-2 and IKONOS satellite imagery data.

Based on this algorithm, we extracted ISA from the high spatial resolution orthophoto data for the state of Rhode Island. The result indicates that 10% of the state land are covered by the ISA. Ten towns have ISA percentage over 20%. Twelve towns have ISA percentage between 10% and 20%. Only sixteen towns in the state have ISA percentage less than 10%. The distribution patterns indicate that the ISA are mainly concentrated along the coastal lines in the southern and the eastern sections of the state. The extracted information of ISA provides the most updated and precise information for coastal and watershed management, as well as for environmental monitoring and modeling.

INTRODUCTION

Impervious surface area (ISA) has emerged as a key paradigm to explain and predict ecosystem health in relationship to watershed development. By definition, urban pavements, such as rooftops, roads, sidewalks, parking lots, driveways and other manmade concrete surfaces are among impervious surface types that feature the urban and suburban landscape. ISA has been considered as a key environmental indicator due to its impacts on water systems and its role in transportation and concentration of pollutants (Arnold and Gibbons 1996). Urban runoff, mostly over impervious surface, is the leading source of pollution in the Nation's estuaries, lakes, and rivers (Arnold and Gibbons 1996, Booth and Jackson 1997). A recently published watershed-planning model predicts that most stream quality indicators decline when watershed ISA exceed 10% (Schueler 2003).

ISA is a critical factor in cycling of terrestrial runoff and associated materials to and within ocean margin waters. Increasing ISA impacts watershed hydrology in terms of influencing the runoff and associated erosion and non-point pollutions. It is necessary to reveal the impact of ISA on runoff and rainfall-runoff relationship.

Reported studies employed hydrologic modeling to quantify the impacts of land-use and land-cover change on hydrological regimes at various scales (Dunn and Mackay, 1995; Ott and Uhlenbrook, 2004). Because of lacking high spatial resolution ISA data, most of current hydrologic models estimated ISA from GIS land-cover data or assigned same value for urban areas (Ott and Uhlenbrook, 2004). However, as ISA is a key parameter in the runoff production, using estimated percentage of ISA instead of precise high spatial resolution ISA data may cause considerable errors in the rainfall-runoff modeling. Therefore, quantifying precisely the percentage of ISA and the spatial locations in landscapes has become increasingly important with growing concern of its impact on the environment (Weng 2001, Civco *et al*. 2002, Dougherty *et al*. 2004, Wang and Zhang 2004).

Classification of remote sensing data is broadly used to extract ISA information. Due to limitations of spectral mixing and spatial resolutions, the accuracy of ISA extraction has always been challenged through classification process. Therefore, efforts have been made to extract ISA from a variety of remote sensing data sources and through modeling. Object-based classification has been developed to conquer the problem existing in the traditional pixel-based image classifications (Baatz and Schäpe, 2000; Shackelford and Davis, 2003). Object-based method is especially suitable for processing high spatial resolution images.

The classifiers used in the pixel-based classification can still be used in object-based methods. For example fuzzy logic is commonly used in object-based classification (Shackelford and Davis, 2003; Baatz *et al.*, 2004; Benz *et al.*, 2004). In order to use fuzzy logic, a rule-base must be established first. Subjective factors may be introduced in the process. Minimum distance and maximum likelihood are reliable classifiers and often used to make comparisons with other algorithms (El-Magd and Tanton, 2003; Reguzzoni *et al.*, 2003; Wang *et al.*, 2004). Minimum distance classifier can be used to build a rule base in fuzzy logic classification. Maximum likelihood classifier is a better one and more useful when prior knowledge is available and statistic criteria are taken into account. In some pixel-based classifiers, such as the maximum likelihood, the variability and relationship between spectral bands of the training pixels are considered. However such information would not be available for a single pixel to be classified in these pixel-based methods. In most of the existed object-based methods, information of variability in the objects and relationship between spectral bands was not considered. Therefore, it will be helpful for an object-based classification to include this type of information.

With the availability of the most recent airborne digital orthophotos, we developed an algorithm using Multivariate Analysis of Variance (MANOVA)-based classification to extract the high spatial resolution ISA. We also tested this algorithm using remote sensing data from different sources. Finally we extracted ISA information for the coastal state of Rhode Island and summarized the spatial distribution patterns of ISA.

METHODOLOGY

Data Preparation

The Rhode Island Statewide Planning Program acquired a set of true color digital orthophoto between 2003 and 2004 through the National Agricultural Imagery Program (NAIP). This 1-meter ground sample distance orthorectified imagery dataset has a horizontal accuracy of within +/- 3 meters of reference digital ortho quarter quads (DOQQS) from the National Digital Ortho Program. The ortho images are projected into Rhode Island State Plane Coordinate System with zone 3800 in U.S. Survey feet. The resulting spatial resolution in this coordinate system is 1 meter (3.28 feet). The dataset has red, green and blue light spectral bands and distributes in GeoTIFF format (Figure 1a).

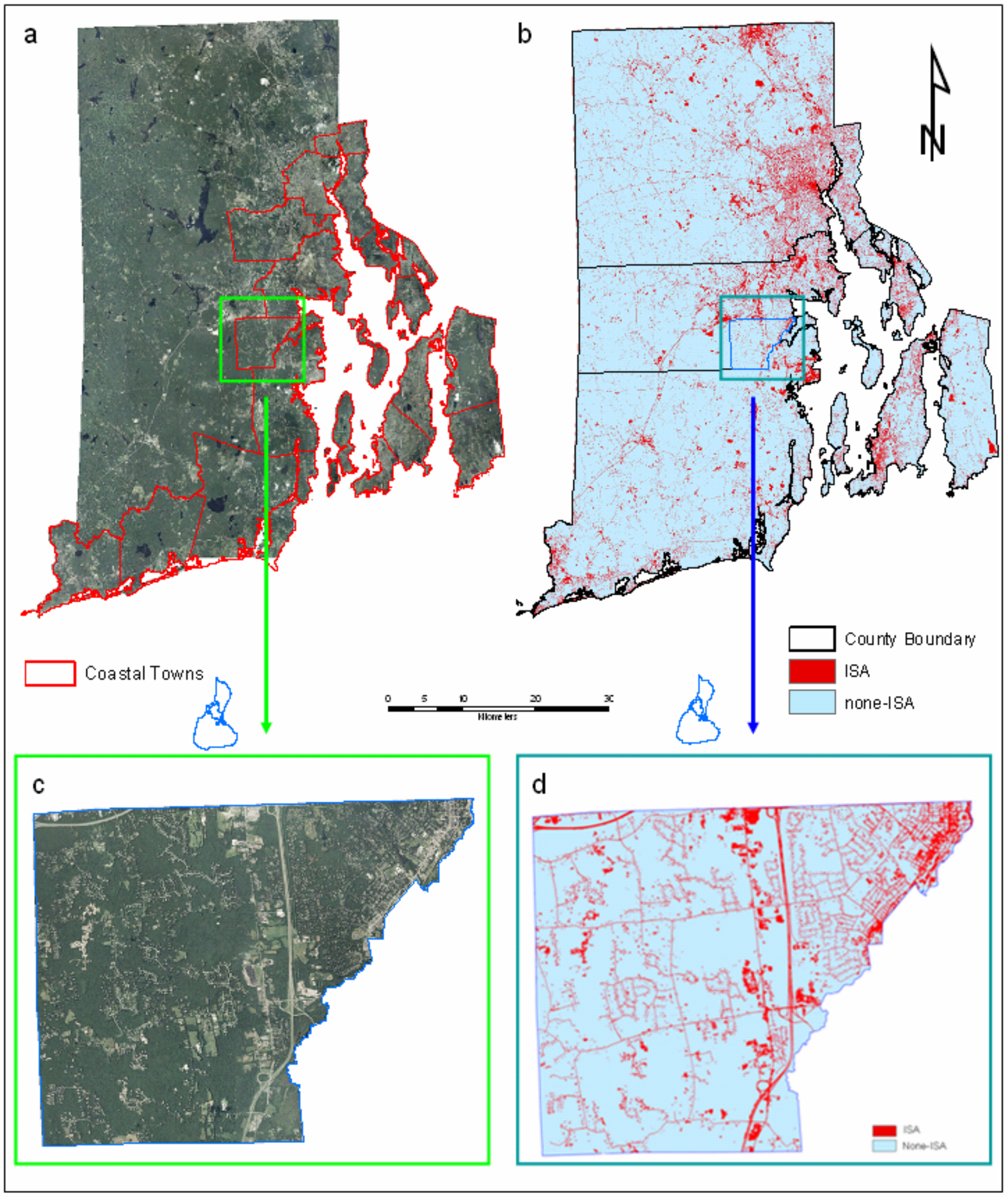

Figure 1. (a) The true color digital orthophoto imagery data with 1-meter spatial resolution for the state of Rhode Island and coastal towns for ISA pattern analysis; (b) The statewide ISA coverage and spatial distributions; (c) and (d) The enlarged orthophoto for East Greenwich township areas and extracted ISA.

We also used the QuickBird-2 satellite data acquired on April 29, 2005 and IKONOS satellite data acquired on December 20, 2003 to test the applicability of the algorithm that we have developed. The QuickBird-2 and IKONOS image data were acquired for quantifying and identifying landscape characteristics related to impervious surface in selected portions of the state. QuickBird-2 image data possess 0.6-m spatial resolution on the panchromatic band and 2.5-m spatial resolution on the multispectral bands. IKONOS image data possess 1-m spatial resolution on the panchromatic band and 4-m spatial resolution on the multispectral bands. The image data were projected into the same map coordinates as orthorectified true-color aerial photos. Both QuickBird-2 and IKONOS data were processed using spatial resolution enhancement. After resolution merge the new dataset of QuickBird-2 possesses 0.6-m spatial resolution with 4 spectral bands (Figure 2a) and IKONOS processes 1-m spatial resolution with 4 spectral bands (Figure 2b).

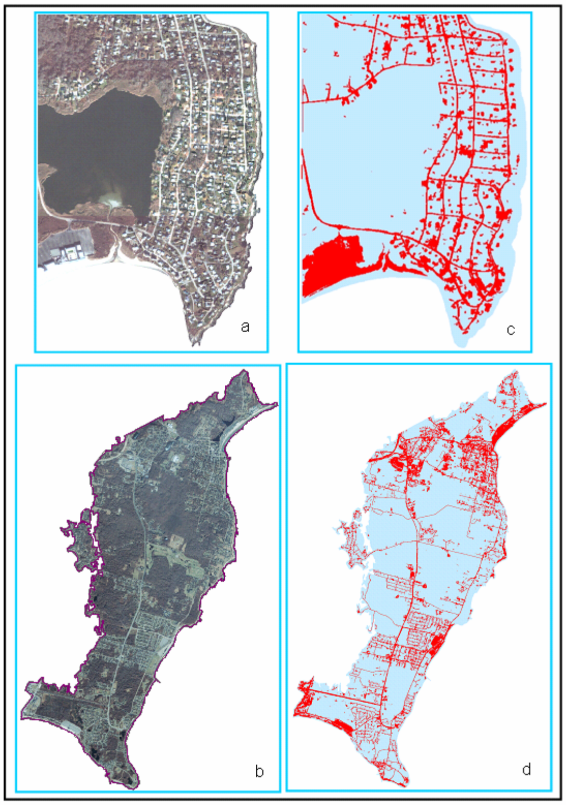

Figure 2. (a) and (c) An example of resolution merged QuickBird-2 image with 0.6-meter spatial resolution and extracted ISA; (b) and (d) An example of resolution merged IKONOS image with 1-meter spatial resolution and extracted ISA.

As texture information can be helpful for spatial information definition (Woodcock and Harward, 1992), we used a 3 x 3 window to extract the variance in the dataset as one of the features in the image segmentation process.

We selected subset areas in Rhode Island for the algorithm testing. The selected testing areas are typical suburban communities with intensive urban developments. ISA are a major concern of these communities in terms of watershed management and environmental monitoring.

MANOVA-based Classification

After the initial and additional segmentation processes, the next step should be the assignment of a class label to each of the regions on segmented image through a classification process. We developed a MANOVA-based classifier on the segmented image in which the relationship between spectral bands and the variability in the training objects and those objects to be classified were taken into account.

This process allowed more information to be exploited in the single object. For example, in the maximum likelihood classification the variance and co-variance matrices of the training samples are used. In most of the existing object-based classification methods, the information of each spectral band is analyzed separately. If the response variables were uncorrelated, these methods would be powerful. However, since spectral bands in remote sensing data are correlated, this MANOVA-based algorithm referenced the spectral distance to exploit such correlations. This process improved the result from univariate analysis that ignored the correlations among spectral bands and assumed independence of response variates. We used following distance equation (Eq. 1) in the MANOVA-based classification algorithm.

$$\begin{cases} T^2 = \dfrac{n_1 n_2}{n_1 + n_2} (\bar{x}_1 - \bar{x}_2)^T S_p^{-1} (\bar{x}_1 - \bar{x}_2) \\ T^2{}_{adj} = \dfrac{n_1 + n_2 - p}{p(n_1 + n_2 - 2)} T^2 \end{cases} \tag{1}$$

where n_1 and n_2 are the numbers of the pixels in the object to be classified and training object; $\bar{x}_1$ and $\bar{x}_2$ are the mean spectral vectors of the object to be classified and training object; S_p is the pooled covariance based on two objects; p is the bands; T^2 is the distance between two objects; and $T^2{}_{adj}$ is the distance with the consideration of the bands and pixels numbers.

We carried out the following process. Firstly, we performed the segmentation using the spectral, shape and texture information in the high spatial resolution remote sensing data and obtained the segmented image. After that, we did the classification based on the MANOVA-based algorithm as follows. We established the training samples for 5 main categories of ISA, forest, grassland, bared soil and water. Each category has several sub-categories. We then recoded the obtained classification result into ISA and none-ISA. Upon finishing the classification we used the existing GIS data through a post-classification process to extract ISA that still could not be identified through the process. We used a rasterized GIS transportation data from Rhode Island Geographic Information System (RIGIS) as a reference to identify the road networks and integrated the road data with output from the classification to obtain the final ISA coverage. The post-classification warrants that the connected ISA is not interrupted and the final result represents the best information from both high spatial resolution remote sensing and GIS data.

Algorithm Extending

It takes 113 scenes of digital orthophotos to cover the state of Rhode Island except Block Island (Figure. 1a). In order to extract the ISA for the state efficiently, we developed an automatic approach based on batch process and applied it on the segmentation and classification process. Firstly, we carried out the segmentations for these scenes using the same set of the parameters as the testing areas. Secondly, we performed the pre-classification stratification according to land-cover and land-use data from the RIGIS, and selected the training objects of certain land-cover types for each subset from pre-classification stratification. We compared and checked these training data according to the covariance matrix of each object, and used the samples with smaller covariance. We then recoded the results into ISA and none-ISA, and finally applied the post-classification to obtain the high spatial resolution ISA for the state.

RESULTS

ISA Extraction

In order to check the accuracy for the extracted ISA from orthophoto, we selected township of East Greenwich to perform the accuracy assessment (Figure 1c and 1d). We used random point sampling method to evaluate the ISA accuracy. We selected 200 test samples and examined the classification accuracies for ISA and none-ISA only. The confusion matrix indicated that this algorithm achieved 94% overall accuracy using orthophoto (Table 1). The omission and commission error were 11% and 1.11% for the ISA, and 1% and 10% for the none-ISA categories, respectively. We also tested the algorithm performance on the QuickBird-2 and IKONOS imageries. Results using QuickBird-2 and IKONOS are shown in Figure 2c and 2d. This algorithm achieved 94% and 91.5% overall accuracies for QuickBird-2 and IKONOS imageries, respectively.

Table 1. Accuracy assessment of MONOVA-based algorithm derived ISA

		MASC Model Derived ISA				
		ISA	none-ISA	Row Total	Omission Error	Accuracy
REFERENCE	ISA	89	11	100	11%	89%
	none-ISA	1	99	100	1%	99%
	Column Total	90	110	200		
	Commission Error	1.11%	10%			Overall 94%

The result of high spatial resolution ISA for the entire state is illustrated in Figure 1b. As the first set of precise statewide ISA data, the result reveals the spatial distribution of ISA, in particular along the coastal line. The results indicate that ISAs cover 10% of the total areas in state of Rhode Island. Five towns including Central Falls, New Port, North Providence, Providence, and Woonsocket, have ISA cover percentage 30%. Five towns including Bristol, East Providence, Pawtucket, Warwick, and West Warwick, have ISA percentage between 20% and 30%. Twelve towns have ISA percentage between 10% and 20%. Only sixteen towns in the state have ISA percentage less than 10% (Table 2).

Table 2. ISA Percentage of inland and coastal townships in Rhode Island.

Inland Towns	Area (ha)	ISA (%)	Coastal Towns	Area (ha)	ISA (%)
Exeter	15130	3	Little Compton	5854	6
Foster	13466	3	Charlestown	9900	6
Glocester	14726	4	S Kingstown	15880	7
Scituate	14201	4	Tiverton	7863	8
W Greenwich	13271	5	Jamestown	2505	9
Hopkinton	11437	5	E Greenwich	4226	11
Burrillville	14760	5	Narragansett	3691	12
Richmond	10556	6	Portsmouth	6115	13
Coventry	16183	8	N Kingstown	11444	14
N Smithfield	6448	9	Barrington	2227	14
Smithfield	7154	9	Westerly	7962	16
Cumberland	7319	13	Warren	1619	16
Johnston	6305	15	Middletown	3420	18
Lincoln	4915	16	Cranston	7492	19
W Warwick	2096	26	Bristol	2559	20
N Providence	1501	31	E Providence	3625	20
Central Falls	334	38	Warwick	9300	24
Woonsocket	2044	40	Pawtucket	2296	26
			Newport	2096	30
			Providence	4873	37
	Average	7		Average	14

Spatial distributions of ISAs are uneven in the state (Figure 1b). ISAs are more intensive along the coastal townships than that in interior areas of the state (Figure 1b and Table 2). Comparisons of the percentage of ISA among costal towns reveal the spatial patterns of ISA cover in these areas (Figure 1b). The percentages of ISA are diverse among the coastal towns (Table 2). ISAs in the coastal townships are relatively higher than that in the inland towns.

Patterns of ISA Distribution

The riparian zones are important in hydrology, ecology and environmental management because of their relationship with soil conservation, biodiversity and water quality. However, with the urban and suburban development ISA along and near the riparian zones increased quickly. In order to understand the spatial patterns of ISA along riparian zones, we built five buffer zones in sizes of 15-, 60-, 120-, 300-, and 600-meter along the major rivers, such as Moshassuck River in northern part of the state and Chipuxet River in southern part of the state, to find spatial distribution of ISA within these zones in coastal towns (Figure 1a). As ISAs along transportation lines form the effective ISA that play more important roles in environmental impacts than isolated ISA, we analyzed the distribution pattern of ISA along the major roads by constructing similar 5 buffer zones as those applied to the major rivers.

Since there are no major rivers in 3 of the coastal towns, we compared the ISA within different sizes of buffer zones for 17 towns. The results of ISA patterns were illustrated in Figure 3. Percentage of ISA in most of the towns shows an increasing trend with the increase of buffered areas. The town of Westerly is an exception, where the ISA show a decreasing trend with the increase of buffer size along the major river (Figure. 3). This is because Westerly has only very limited areas that are covered by the river buffers. The decreasing trend may not reflect the real pattern of ISA cover within the township areas.

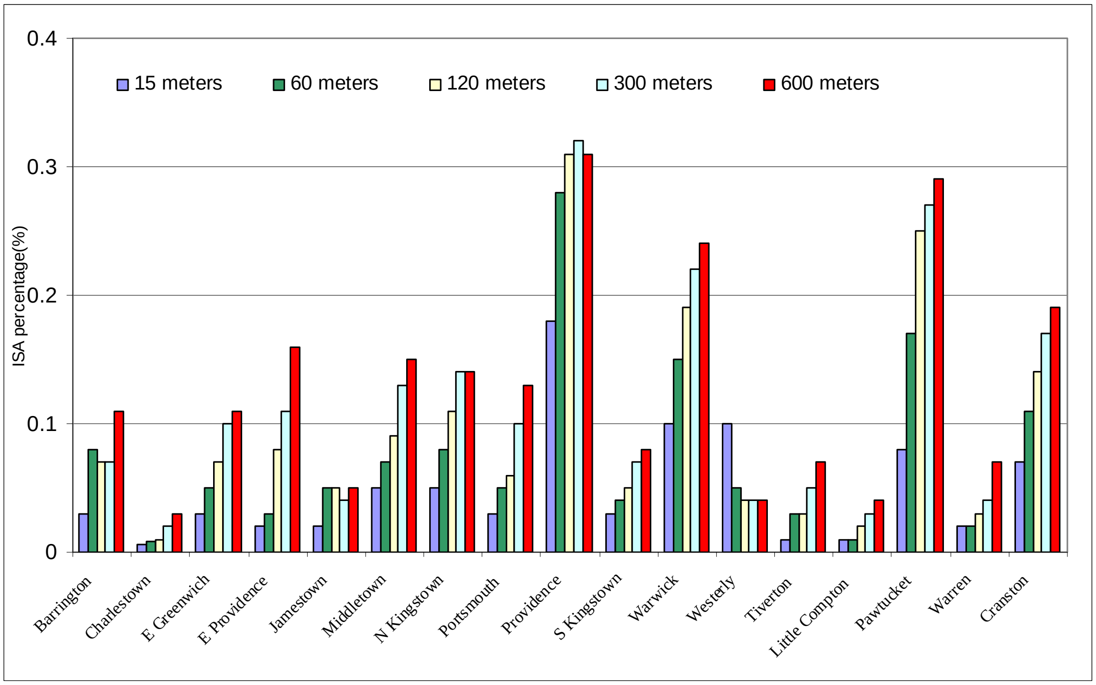

Figure 3. ISA Percentage in 5 buffer zones along the major rivers in coastal towns.

Figure 4 shows the ISA along the major roads with varied sizes of buffered areas. Different from the patterns observed in the riparian zones, the percentage of ISA shows a decreasing trend with the increase of buffered areas, which indicates that most of the ISAs distribute along the road networks. The rate of decreasing in percentage of ISA is reduced as the buffered areas enlarged.

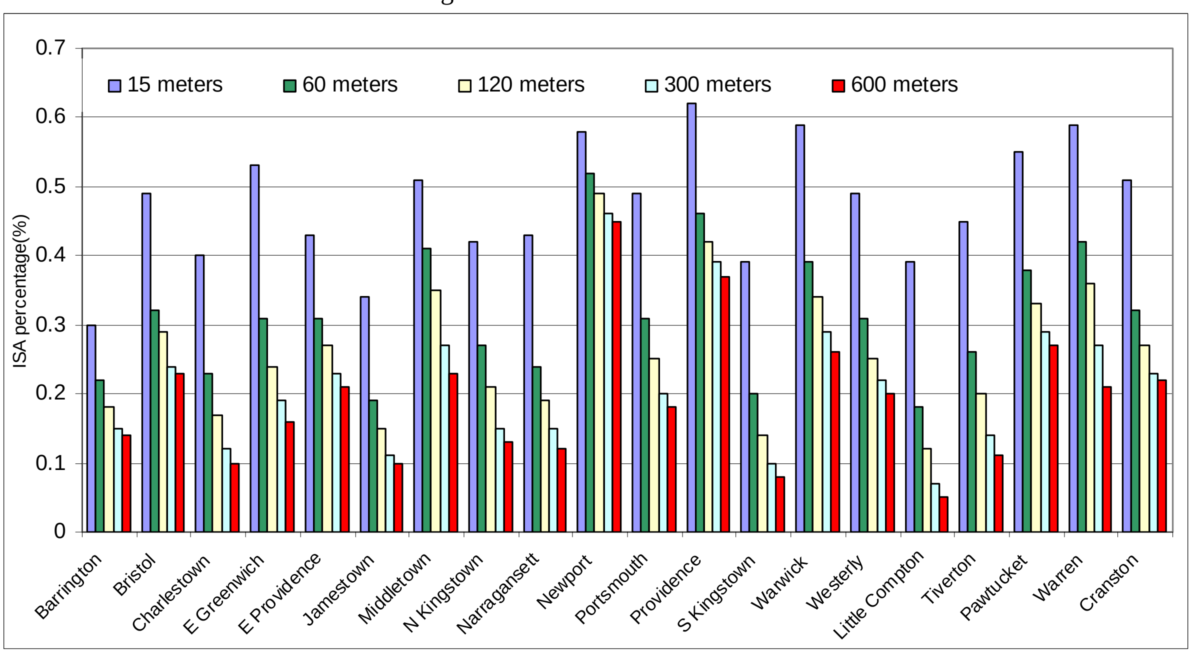

Figure 4. ISA Percentage in 5 buffer zones along the major roads in coastal towns.

CONCLUSIONS AND DISCUSSIONS

This study developed a MANOVA-based classification algorithm on the segmented images. The variability within the object and the relationship between the spectral bands were taken into account. Compared with the pixel-based method, this algorithm achieved more precise and accurate information on ISA distribution. In pixel-based methods, the variability and relationship between spectral bands of the training samples are taken into account in some classifiers such as maximum likelihood. There was no such information for a single pixel to be classified in those methods. In most of existing object-based methods, the relationships between different spectral bands were not considered. Because of the correlations among different spectral bands in remote sensing data, it is helpful to consider this correlation information in the data process. The MANOVA-based algorithm exploits the correlations of the spectral bands to explain the spectral distance between the training objects and those objects to be classified.

The algorithm is successful in extraction of ISA from high spatial resolution airborne true color digital Orthophoto, as well as from space borne multispectral images. True color Orthophoto data are more common among state agencies and have been widely used by the general public. The QuickBird-2 and IKONOS data have advantages in multispectral coverage. The digital Orthophoto, spatially enhanced QuickBird-2 and IKONOS data possess comparable spatial resolution. The results from multiple testing areas, as well as from the entire state with different landscape and ISA characteristics verified that this algorithm is applicable and robust. Therefore, the algorithm can meet the requirements in high spatial resolution ISA extraction.

This study provided the high spatial resolution ISA information for the state of Rhode Island using the developed algorithm. This is the first statewide high spatial resolution ISA dataset in Rhode Island. The data are valuable for land management, planning, and for ecological and hydrological modeling to determine the impacting effects of land use patterns on coastal environment and watersheds of the state. The distribution patterns obtained from this study indicate that ISAs are mainly concentrated along the coastal areas in the southern and eastern sections of the state. The percentages of ISA are highest within the nearest buffer along the road networks. ISAs are in increasing trends with the increase of buffer size along the riparian zones. The impact of ISA on water quality, particularly for the towns that have high percentage of ISA cover, needs to be considered in development and planning.

ACKNOWLEDGEMENTS

This study was funded by the Rhode Island Agricultural Experimental Station (RI00H330). The QuickBird-2 data came from another project funded by the Institute for the Application of Geospatial Technology, and the IKONOS data came from ASPRS GeoEye Award.

REFERENCES

Arnold, C.A. Jr., and C.J. Gibbons (1996). Impervious surface coverage: the emergence of a key urban environmental indicator. *Journal of the American Planning Association*, 62(2): 243-258.

Baatz, M. and A. Schäpe (2000). Multiresolution segmentation: an optimization approach for high quality multi-scale image segmentation. In: *Angewandte Geographische Informationsverarbeitung XII* (Strobl, J. and T. Blaschke, editors), Wichmann-Verlag, Heidelberg, pp. 12-23.

Baatz, M., U. Benz, S. Dehghani, M. Heynen, A. Höltje, P. Hofmann, I. Lingenfelder, M. Mimler, M. Sohlbach, M. Weber, and G. Willhauck (2004). eCognition User Guide, URL: http://www.definiens-imaging.com, Definiens Imaging, München, Germany (last date accessed: 25 July 2005).

Benz, U., P. Hofmann, G. Willhauck, I. Lingenfelder, and M. Heynen (2004). Multi-resolution, object-oriented fuzzy analysis of remote sensing data for GIS-ready information. *ISPRS Journal of Photogrammetry & Remote Sensing*, 58 (3-4): 239– 258.

Booth, D.B., and C.R. Jackson (1997). Urbanization of aquatic systems: Degradation thresholds, stormwater detection, and the limits of mitigation. *Journal of American Water Resources Association*, 35(5): 1077-1090.

Civco, D.L., J.D. Hurd, E.H. Wilson, C.L. Arnold, and S. Prisloe (2002). Quantifying and Describing Urbanizing Landscapes in the Northeast United States. *Photogrammetric Engineering & Remote Sensing*, 68(10): 1083-1090.

Dougherty, M., L. D. Randel, J. G.. Scott, A. J. Claire, and G. Normand (2004). Evaluation of Impervious Surface

Estimates in a Rapidly Urbanizing Watershed. *Photogrammetric Engineering & Remote Sensing*, 70(11): 1275–1284.
Dunn, S.M. and R. Mackay (1995). Spatial variation in evapotranspiration and the influence of land use on catchment hydrology. *Journal of Hydrology*, 171(1-2): 49-73.
El-Magd, I. A., and T.W. Tanton (2003). Improvements in land use mapping for irrigated agriculture from satellite sensor data using a multi-stage maximum likelihood classification. *International Journal of Remote Sensing*, 24(21): 4197-4206.
Ott, B. and S. Uhlenbrook (2004). Quantifying the impact of land-use changes at the event and seasonal time scale using a process-orientated catchment model. *Hydrology and Earth System Sciences*, 8(1): 62–78.
Reguzzoni, M., F. Sanso, G. Venuti, and P. A. Brivio (2003). Bayesian classification by data augmentation. *International Journal of Remote Sensing*, 24(20): 3961-3981.
Schueler, T. (2003). *Impacts of Impervious Cover on Aquatic Systems*. Center for Watershed Protection (CWP), Ellicott City, MD., 142p.
Shackelford, A.K and C. H. Davis (2003). A combined fuzzy pixel-based and object-based approach for classification of high-resolution multispectral data over urban areas. *IEEE Transactions on Geoscience & Remote Sensing*, 41(10): 2354-2363.
Wang, L., W. P. Sousa, and P. Gong (2004). Integration of Object-based and Pixel-based Classification for Mapping Mangroves with IKONOS Imagery. *International Journal of Remote Sensing*, 25(1): 1-14.
Wang, Y. and X. Zhang (2004). A SPLIT Model for Extraction of Subpixel Impervious Surface Information. *Photogrammetric Engineering and Remote Sensing*, 70: 821-828.
Weng, Q. H. (2001). Modeling Urban Growth Effects on Surface Runoff with the Integration of Remote Sensing and GIS. *Environmental Management*, 28(6): 737-748.
Woodcock, C. E., and V. J. Harward (1992). Nested-Hierarchical Scene Models and Image Segmentation. *International Journal of Remote Sensing*, 13(16): 3167-3187.